Recent CP violation and lifetime results from CMS

Vladimir Sergeychik[1,2,*], on behalf of the CMS Collaboration

[1] Moscow Institute of Physics and Technology, Russia
[2] P.N. Lebedev Physical Institute of the Russian Academy of Sciences, Russia

Abstract. Recent results on CP violation in charm and beauty sector, as well as lifetime measurements, by the CMS experiment at the LHC are presented. The first measurement of CP violation in charm by CMS is reported, as well as the most precise measurement of effective lifetime $\tau(B_s^0 \to J/\psi K_S^0)$ and the first evidence for CP violation in the $B_s^0 \to J/\psi\phi(1020) \to \mu^+\mu^- K^+ K^-$ decay. The analyses are based on 13 TeV proton-proton collision data.

1 Introduction

Baryon asymmetry of the universe (BAU) remains one of the great mysteries of modern physics. The noninvariance of fundamental interactions under the combined charge-parity (CP) transformation is one of the necessary conditions for generation of observed BAU [1]. The standard model accounts for CP violating effects via a single phase in the Cabibbo–Kobayashi–Maskawa (CKM) quark mixing matrix [2, 3]. Nevertheless, the magnitude of CP violating effects within the SM is insufficient to account for the observed BAU [4], which means that beyond the SM mechanisms for CP violation must exist. Moreover, all observables in CP violation studies are predicted with great precision. All these factors make the CP violation measurements sensitive to probing new physics.

The CMS Experiment [5] at the CERN LHC is a general purpose detector and is able to perform a vast range of physics studies, including flavor physics. Excellent tracking system [6], as well as a large amount of data collected and a refined trigger strategy allow the CMS to compete with the specialized flavor physics experiments (like LHCb, Belle, BaBar) and to actively contribute to the heavy hadron physics [7–10].

In the present work, three recent results from the CMS Collaboration are reported: the search for direct CP violation in $D^0 \to K_S^0 K_S^0$ decay [11], the effective lifetime of the $B_s^0 \to J/\psi K_S^0$ decay measurement [12] and the measurement of time-dependent CP violation in the $B_s^0 \to J/\psi\phi(1020) \to \mu^+\mu^- K^+ K^-$ decay [13]. All these studies are crucial to shed light on CP violation phenomenology.

2 Search for CP violation in $D^0 \to K_S^0 K_S^0$

Charmed meson decays are the only meson decays involving an up-type quark where CP violation can be studied, however, in contrast to the K and B systems, CP violation in charm mesons is severely suppressed by the Glashow–Iliopoulos–Maiani mechanism [14] and by

*e-mail: vladimir.sergeychik@cern.ch

the magnitude of the CKM elements [2, 3]. Given the strong Standard Model suppression, an observation of a significant CP violation in D meson decays may indicate a contribution from new physics mechanisms. The $D^0 \to K^0_S K^0_S$ decay proceeds through the tree-level exchange diagram and penguin annihilation diagrams, which are shown on the Fig. 1. Theoretical predictions indicate similar amplitudes and different phases for the two diagrams, which can result in CP violation in this channel as large as a few percent [15] and therefore possibly within reach of current experiments.

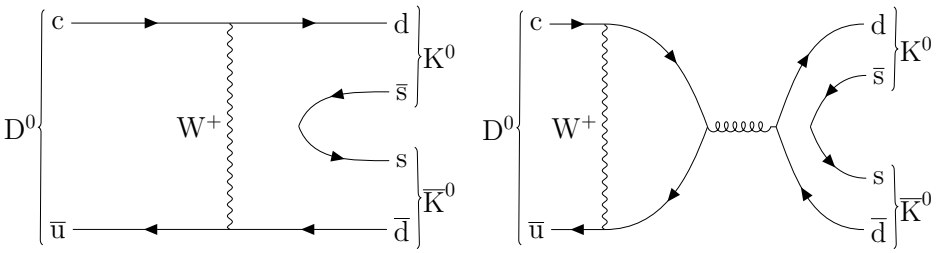

Figure 1. The decay of neutral charm meson to two neutral kaons: exchange (left) and penguin annihilation (right) diagrams [11].

The CP asymmetry A_{CP}, for the $D^0 \to K^0_S K^0_S$ decay, is defined as

$$A_{CP}(K^0_S K^0_S) = \frac{\Gamma(D^0 \to K^0_S K^0_S) - \Gamma(\bar{D}^0 \to K^0_S K^0_S)}{\Gamma(D^0 \to K^0_S K^0_S) + \Gamma(\bar{D}^0 \to K^0_S K^0_S)}. \tag{1}$$

The current world-average of this quantity is = $(-1.9 \pm 1.1)\%$ [16] with the most significant contribution coming from the LHCb collaboration measurement [17].
In the CMS analysis the flavor of neutral D is determined by the pion charge found from the decays $D^{*+} \to D^0\pi^+$ and $D^{*-} \to \bar{D}^0\pi^-$. The physical asymmetry from Eq. 1 depends on the $D^{*\pm}$ production asymmetry, on the asymmetry of the detection efficiency, and on the "raw" asymmetry, which indicates the difference in the number of reconstructed D^{*+} and D^{*-} candidates. Taking these three asymmetries, the expression from the Eq. 1 can be rewritten in the following way:

$$A_{CP} \approx A^{raw}_{CP} - A^{pro}_{CP} - A^{det}_{CP}, \tag{2}$$

The measurements of A^{pro}_{CP} and A^{det}_{CP} might contribute to the systematic uncertainty, therefore, to reduce this impact, the analysis measures the difference of A_{CP} between the $D^0 \to K^0_S K^0_S$ (signal channel) and $D^0 \to K^0_S \pi^+\pi^-$ (reference channel): these channels have similar kinematics and topology, hence, the measurement of ΔA_{CP} (defined in Eq. 4) allows to obtain the statistically-driven observable with negligible systematic uncertainty.

$$\Delta A_{CP} \equiv A_{CP}(K^0_S K^0_S) - A_{CP}(K^0_S \pi^+\pi^-) = A^{raw}_{CP}(K^0_S K^0_S) - A^{raw}_{CP}(K^0_S \pi^+\pi^-) \tag{3}$$

The analysis uses proton-proton collisions data recorded by the CMS detector during the CERN LHC Run 2 in 2018 at $\sqrt{s}$ = 13 TeV. It utilizes the B parking data set [18], collected with a set of single-muon triggers with different minimum thresholds on the muon transverse momentum.
One of the most significant sources of charm quark production is the decay of the heavier *b*-quark. Therefore, among all the events in this analysis, those associated with the decays of *b*-hadrons are of great interest. In 2018, a B parking strategy for muon triggers was employed

on the CMS detector: event recording only occurred if the detached muon had a sufficiently large transverse momentum (p_T); depending on the trigger, a p_T value greater than 5-12 GeV was required, thus collecting events associated with $b \to \mu X$ decays. It is well known that in semi-leptonic decays of b-hadrons [16], a c-quark is almost always produced. Therefore, the B-parking dataset contains $O(10^{10})$ events with charm hadrons, each possessing sufficiently high momentum, making it well-suited for precision measurements in the charm sector, particularly for measuring the CP violation parameter.

The reconstruction process of the studied channel starts with the selection of five final tracks of charged pions. In reference channel, it is required that the probability of successful reconstruction of two of them into K^0_S mass exceeds 1 %. In signal channel, it is also required that the other two tracks are successfully reconstructed into K^0_S. Then, from the obtained virtual K^0_S tracks and two pion tracks (or from another virtual K^0_S track in the case of signal channel), the D^0 decay vertex is reconstructed. In the final stage, the reconstructed D^0 vertex is combined with the fifth pion track to form the common vertex of $D^*(2010)^{\pm}$. The objects of study are the numbers of events for the decays of $D^*(2010)^-$ and $D^*(2010)^+$. Likewise, additional selection criteria are implied in order to minimize the statistical uncertainty of ΔA_{CP} measurement [11].

To extract the raw CP asymmetry in reference channel, a simultaneous binned extended maximum likelihood fit is performed on the invariant mass distributions $m(D^0\pi)$ of D^{*+} and D^{*-} candidates. The results of the fit to the $m(D^0\pi)$ distributions are presented in Fig. 2 and Table 1.

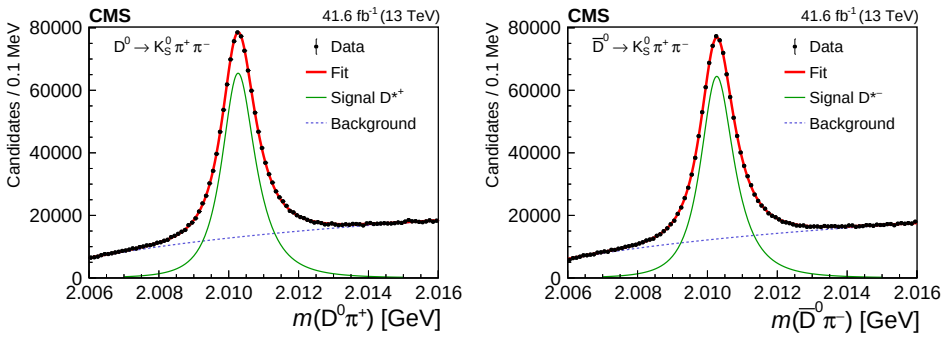

Figure 2. The $D^0\pi^+$ (left) and $\bar{D}^0\pi^+$ (right) invariant mass distributions for the $K^0_S\pi^+\pi^-$ channel, with the result of the fit to both distributions [11].

In signal channel, to reduce the statistical uncertainty arising from the signal channel yield, which is the dominant uncertainty in the analysis, the signal extraction is performed using a 2D unbinned maximum likelihood (UML) fit performed simultaneously on the $D^*(2010)^+$ and $D^*(2010)^-$ samples to the distribution of $m(D^0\pi)$ vs. $m(K^0_S K^0_S)$. The results of the fit are presented in Fig. 3 and Table 1.

The measured difference in the asymmetries is largely insensitive to systematic uncertainties. The most significant sources of them are the uncertainty in fit model choice, fit range and the matching of reference and signal channels distributions.

Combining systematic and statistical uncertainty, the difference in the CP asymmetries between $D^0 \to K^0_S K^0_S$ and $D^0 \to K^0_S\pi^+\pi^-$ is measured to be [11]:

$$\Delta A_{CP} \equiv A_{CP}(K^0_S K^0_S) - A_{CP}(K^0_S\pi^+\pi^-) = (6.3 \pm 3.0 \pm 0.2)\,\% \tag{4}$$

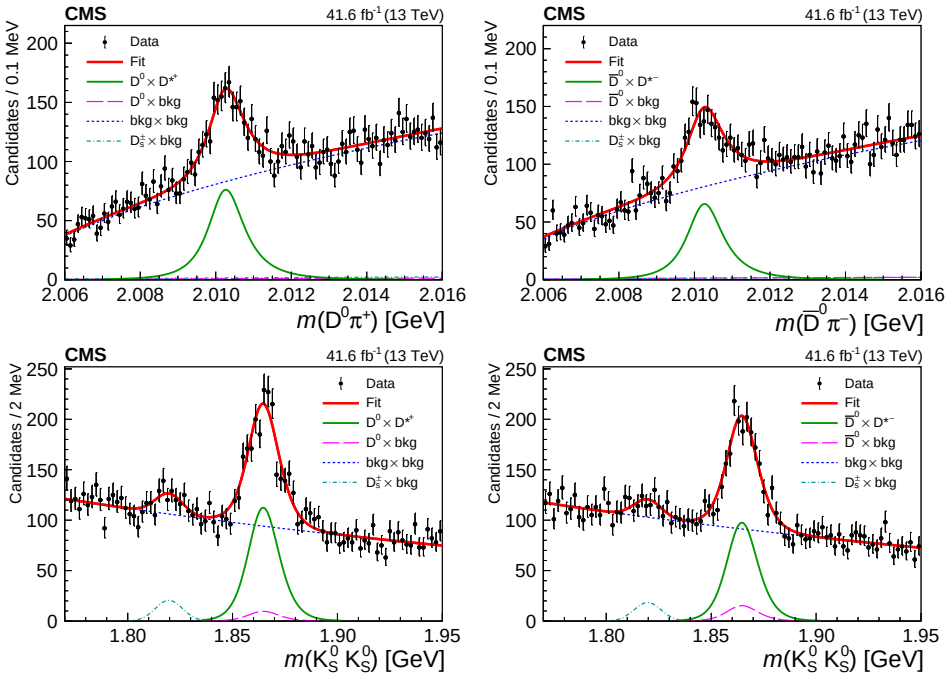

Figure 3. The invariant mass distributions for $D^*(2010)^+$ candidates (left) and $D^*(2010)^-$ candidates (right), with the $m(D^0\pi)$ distributions in the upper row and the $m(K^0_S K^0_S)$ distributions in the lower row. Projections of the simultaneous 2D fit are also shown [11].

Table 1. Results of the fit to the selected $D^*(2010)^+ \to D^0\pi^+$ and $D^*(2010)^- \to \bar{D}^0\pi^-$ candidates. The $D^*(2010)^\pm$ signal yields N given in the second column are used in the evaluation of ΔA_{CP}^{raw}. The uncertainties are statistical only [11].

Decay	N
$D^*(2010)^+ \to D^0(\to K^0_S\pi^+\pi^-)\pi^+$	944 800 ± 3 500
$D^*(2010)^- \to \bar{D}^0(\to K^0_S\pi^+\pi^-)\pi^-$	930 150 ± 3 400
$D^*(2010)^+ \to D^0(\to K^0_S K^0_S)\pi^+$	1095 ± 46
$D^*(2010)^- \to \bar{D}^0(\to K^0_S K^0_S)\pi^-$	951 ± 44

Using the world-average value of = $(-0.1 \pm 0.8)\%$ [16], we report the measurement [11]

$$A_{CP}(K^0_S K^0_S) = (6.2 \pm 3.0 \pm 0.2 \pm 0.8)\%, \tag{5}$$

where the three uncertainties represent the statistical uncertainty, the systematic uncertainty, and the uncertainty in the measurement of the asymmetry in the $D^0 \to K^0_S\pi^+\pi^-$ decay. The measured value is consistent with no CP violation within 2.0 s. d. Likewise, it is consistent with the LHCb [17] measurement at the level of 2.7 s.d., respectively. This is the first CMS search for CP violation in the charm sector, paving the way for future measurements with more data, using new techniques, and in other channels.

3 Measurement of effective lifetime of the $B_s^0 \to J/\psi K_S^0$

Measurements using b-hadron decays have greatly enhanced our understanding of the standard model flavor sector. The oscillations of B^0 and B_s^0 mesons make them particularly valuable for the verification of the SM predictions for the CP violation. Neutral B mesons are produced as flavor states but travel as the mass eigenstates (light and heavy states), which are a linear combination of the two flavor states. When CP violation is not present in the flavor mixing, the mass eigenstates align with CP eigenstates. These mass eigenstates can have different lifetimes, which may differ from the average B meson lifetime.
In this analysis, the effective lifetime of the B_s^0 meson in its decay to $J/\psi K_S^0$ is measured. The existence of a nonzero decay width difference, denoted as $\Delta\Gamma_s$, in the B_s^0 system enables the extraction of information regarding the mass eigenstate rate asymmetry, $A_{\Delta\Gamma_s}$. The $J/\psi K_S^0$ state is (almost) a CP-odd state [19], which allows the measurement of the B_s^0 heavy-state lifetime provided that CP violation in mixing is negligible. Figure 4 shows the diagrams for the decay modes $B_s^0 \to J/\psi K_S^0$ and $B^0 \to J/\psi K_S^0$. These decays are related through the U-spin flavor symmetry. Using this symmetry, the $B^0 \to J/\psi K_S^0$ decay can be used to determine the hadronic penguin parameters that are important for a precision measurement of $\sin 2\beta$, where β is one of the angles from the CKM unitarity triangle [20].

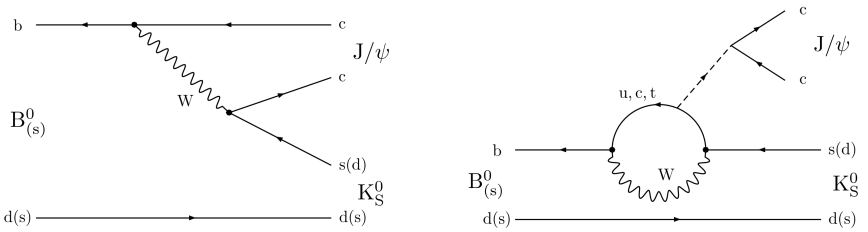

Figure 4. The tree-level (left) and penguin (right) diagrams for the decay $B_s^0 \to J/\psi K_S^0$ [12].

The effective lifetime is theoretically defined as the time expectation value of the untagged decay rate, where untagged means that no requirements are made that would bias one B_s^0 mass eigenstate over the other. The effective lifetime is connected to the $A_{\Delta\Gamma_s}$:

$$\tau\left(J/\psi K_S^0\right)^{eff} = \frac{\tau_B^0}{1-y_s^2}\left(\frac{1+2A_{\Delta\Gamma_s}y_s+y_s^2}{1+A_{\Delta\Gamma_s}y_s}\right), \tag{6}$$

where y_s is the normalized decay width difference, defined as $y_s = \tau_{B_s^0}\frac{\Delta\Gamma_s}{2}$, $\Delta\Gamma_s$ is the decay width difference between the heavy and light B_s^0 mass eigenstates, and $\tau_{B_s^0}$ denotes the mean B_s^0 lifetime. The standard model predictions for this figure are [16]:

$$\tau\left(J/\psi K_S^0\right)^{eff}\Big|_{\text{SM}} = 1.62 \pm 0.02\text{ps}, \tag{7}$$

The previous measurement by the LHCb experiment [21] using the same decay mode reported a value of $\tau\left(J/\psi K_S^0\right)^{eff} = 1.75 \pm 0.12\ (\text{stat}) \pm 0.07\ (\text{syst})$ ps, consistent with the SM calculation.
Data used in the analysis were recorded during stable LHC beam periods, corresponding to an integrated luminosity of 140 fb^{-1} [22], collected by the CMS experiment during 2016–2018 in proton-proton collisions at $\sqrt{s} = 13$ TeV. Events of interest are selected using a two-tiered trigger system. The first level, uses information from the calorimeters and muon detectors to

select events at a rate of around 100 kHz within a fixed latency of 4 μs and the second level reduces the event rate to around 1 kHz before the data storage.

The reconstruction process commences by identifying two muons with opposite charges, which must correspond to those that triggered the readout. These muon pairs are fitted to a common vertex and retained for further use if the fit probability is greater than 0.5%. For the offline reconstruction, the decay $B^0_{(s)} \to J/\psi K^0_S$ is reconstructed using the J/ψ meson decay to $\mu^+\mu^-$ and K^0_S meson decay to $\pi^+\pi^-$. The $\pi^+\pi^-$ and $\mu^+\mu^-$ are also required to be within 2.5 reconstructed resolution from the mean of K^0_S and J/ψ respectively. The contamination in the K^0_S candidates from $\Lambda \to p\pi^-$ is removed using the Armenteros-Podolansky method [23]. Then, reconstructed K^0_S and dimuon are fitted into common vertex. Likewise, additional selection criteria are used [12]. The channel $B^0 \to J/\psi K^0_S$ is used as a control channel.

To extract the information regarding the decay lifetime, a 2D UML fit to $m(J/\psi K^0_S)$ vs. t is used, where proper decay time is defined as:

$$t = \frac{L_{xy} m}{p_{\mathrm{T}}}, \tag{8}$$

where m and p_{T} are the invariant mass and transverse momentum of the B candidate, respectively, and L_{xy} is the decay length in the transverse direction between the production and decay vertices. The uncertainty in the proper decay time is determined by propagating the uncertainties in the decay length, invariant mass, and momentum of the B candidate.

To reduce backgrounds, a multivariate selection is employed, based on a boosted decision tree (BDT). The BDT classifier uses two input samples containing signal and background decays, respectively. The optimization of the BDT threshold is done by minimizing the uncertainty in the proper lifetime measurement based on studies using toy models. The BDT discriminant is required to be greater than 0.61 (0.60) for events collected in 2016 and 2018 (2017) [12].

The measured invariant mass and proper decay time distributions are shown in Fig. 5, along with the combined projections of the 2D UML fit, in the full fit range.

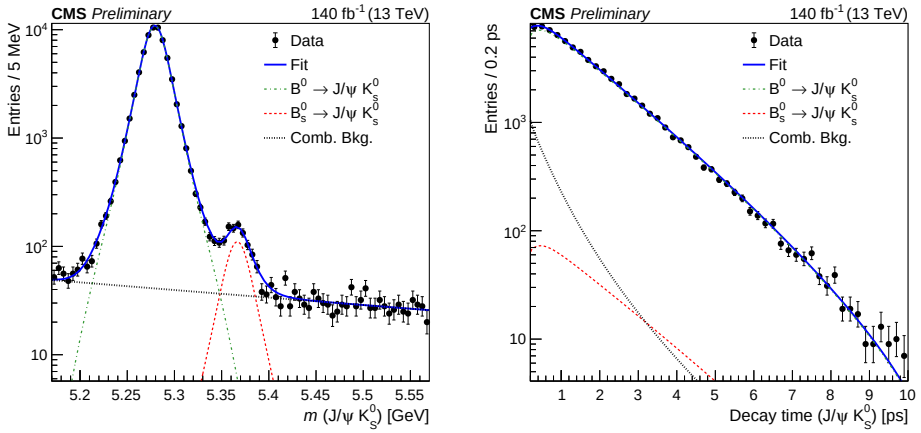

Figure 5. The proper decay time distribution from data (points) for events in the B^0_s signal region with invariant mass $J/\psi K^0_S$ in the range 5.34 – 5.42GeV. The vertical bars on the data points indicate the statistical uncertainty. The dashed, dotted-dashed, dotted, and solid lines show the B^0_s signal, B^0 control channel, combinatorial background, and total fit contributions, respectively [12].

The systematic uncertainties account for the difference between the measured B^0 lifetime and the world-averaged quantity of the value, the limited simulation samples statistics, the efficiency model, and, finally, the uncertainty in choice of the fit model.
The measured yields of the B_s^0 and B^0 signals are found to be 727 ± 35 and 68460 ± 270 respectively, where the uncertainties are statistical only. The final result for $B_s^0 \to J/\psi K_S^0$ effective lifetime is [12]

$$\tau\left(J/\psi K_S^0\right)^{eff} = 1.59 \pm 0.07\ (\text{stat}) \ \pm 0.03\ (\text{syst})\ \text{ps}. \tag{9}$$

The result is consistent with SM calculations and is compatible with the LHCb results [21] at the level of 2.1 s.d.

4 Measurement of time-dependent CP violation in B_s^0 mesons

The decay of B_s^0 mesons to a CP eigenstate $c\bar{c}s\bar{s}$ offer significant opportunities for the study of CP violation in the interference between decays with and without mixing. In this analysis, the CP observable of weak phase angle ϕ_s, as well as is extracted from the study of the decay $B_s^0 \to J/\psi\ (\to \mu^+\mu^-)\ \phi(1020)\ (\to K^+K^-)$. This analysis is performed on CMS Run 2 data, collected at $\sqrt{s} = 13$ TeV during 2017–2018. This work benefits from a larger data sample and a new pioneering flavor tagging algorithm, which in combination lead to the largest effective statistics ever used for a single measurement of ϕ_s.
The $B_s^0 \to J/\psi\ \phi(1020)$ final state is a mixture of CP eigenstates, which requires an amplitude analysis to separate the CP-odd and the CP-even components. A time-dependant angular analysis is performed in the transversity basis by measuring the decay angles of the final-state particles $\Theta = (\theta_T, \psi_T, \phi_T)$ and the proper decay length t of the reconstructed B_s^0 candidate. The illustration of the e three decay angles is provided in Fig. 6.

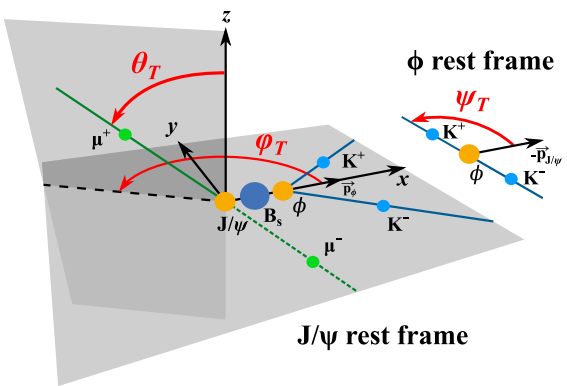

Figure 6. Definition of the three angles θ_T, ψ_T, and φ_T describing the $B_s^0 \to J/\psi\ \phi \to \mu^+\mu^- K^+K^-$decay [13].

The decay rate used to describe the distribution of the final state particles consists of a function $\mathcal{F}(\Theta, ct, \alpha)$, as in Ref. [25]:

$$\frac{\mathrm{d}^4\Gamma_s\left(\mathrm{B_s^0}\right)}{\mathrm{d}\Theta \mathrm{d}(ct)} = \mathcal{F}(\Theta, ct, \alpha) \propto \sum_{i=1}^{10} O_i(ct, \alpha) g_i(\Theta), \tag{10}$$

where O_i are time-dependent functions, g_i are angular functions, and α is a set of physics parameters. The functions $O_i(ct, \alpha)$ are defined as:

$$O_i(ct, \alpha) = N_i e^{-\Gamma_s t}\left[a_i \cosh\left(\frac{\Delta\Gamma_s t}{2}\right) + b_i \sinh\left(\frac{\Delta\Gamma_s t}{2}\right) + c_i \cos(\Delta m_s t) + d_i \sin(\Delta m_s t)\right]. \quad (11)$$

The functions $g_i(\Theta)$ and the parameters N_i, a_i, b_i, c_i, and d_i are defined in Ref. [13]. The physics parameters are the weak phase ϕ_s; the decay width (absolute mass) difference $\Delta\Gamma_s$ (Δm_s) between the light and heavy B_s^0 mass eigenstates; their average decay width Γ_s; the CPV parameter $|\lambda|$; the perpendicular, longitudinal, and parallel transversity amplitudes $A_0, A_\parallel$, and $A_\perp$; and the respective strong phases $\delta_0, \delta_\parallel$, and $\delta_\perp$. The model for the decay of the B_s^0 meson is depicted in Eq. 10, whereas the model for the decay of the $\bar{B}_s^0$ meson is derived by inverting the signs of the c_i and d_i terms in Eq. 11.

The data for this analysis are collected with two independent triggers: "*muon-tagging*", that requires a $J/\psi \to \mu^+\mu^-$ candidate along with an additional muon potentially usable for flavor tagging and "*standard*", that requires to present a displaced $J/\psi \to \mu^+\mu^-$ candidate in conjunction with a $\phi \to K^+K^-$. More information about the selection can be found in the Ref. [13].

The flavor of the B_s^0 candidate at production is determined by a novel flavor tagging framework which consists of four separate tagging algorithms ("taggers"): opposite-side (OS) muon, OS electron, OS jet, and same-side (SS). The OS approach relies on the predominant production of b quarks in $b\bar{b}$ pairs. Thus, the initial flavor of the B_s^0 meson can be inferred by determining the flavor of the other ("OS") b quark in the event. On the other hand, SS taggers take advantage of the charge correlations reflecting underlying flavor content between the signal b meson and nearby particles produced in its hadronization. Each algorithm is constructed to produce a tagging decision $\xi_{\text{tag}} = 0, +1, -1$, if the candidate is classified as untagged, B_s^0, or $\overline{B}_s^0$, respectively, and an estimation of the mistag probability $\omega_{\text{tag.}}$. The fraction of tagged events is called "tagging efficiency" (ε_{tag}), while ω_{tag} can be used to evaluate the dilution $\mathcal{D} \equiv 1 - 2\omega_{\text{tag}}$, an indication of performance degradation. Taking into account the dilution, the "tagging power" $P_{\text{tag}} \equiv \varepsilon_{\text{tag}}\mathcal{D}^2$ acts as the effective tagging efficiency and can be used to evaluate the effective statistical power of a data sample. All four taggers are deployed in the standard data sets, while only the OS muon algorithm is used in the muon-tagging data sets. To maximize performance, ω_{tag} is evaluated on a per-event basis by dedicated DNNs. All DNNs are developed using the KERAS library [26] in simulated events. In all optimization cases, the DNNs employ the cross-entropy loss function combined with the Adam optimizer [27].

The event mistag probability, as estimated by the tagging algorithms, undergoes calibration utilizing a self-tagging data sample of $B^+ \to J/\psi K^+$, where the kaon's charge corresponds to the flavor of the $B^\pm$ meson. The calibration procedure is executed by comparing the measured mistag fraction (ω_{meas}) with the ω_{tag} predicted by the taggers. The flavor tagging framework is validated with extensive studies on simulations and the $B^0 \to J/\psi K^*(892)^0 \to \mu^+\mu^- K^+\pi^-$. The physics parameters of interest are extracted with a simultaneous UML fit to the B_s^0 data sets using seven observables as input: $m_{B_s}, ct, \sigma_{ct}, \cos\theta_T, \cos\psi_T, \varphi_T$, and $\omega_{\text{tag.}}$. The list of the determined physical parameters from the fit is presented on the Tab. 2. The measured number of $B_s^0 \to J/\psi\phi$ signal events from the fit is 491270 ± 950, while the effective tagged statistics, represented as $N_{B_s^0} \cdot P_{\text{tag}}$, amount to approximately 28000, which is the highest ever used for this channel in a single measurement.

The systematic uncertainties are either related to the parameters of the efficiency and calibration functions (these uncertainties are evaluated by either sampling the parameters based

on their uncertainties or re-sampling a data sample) or account for potential biases resulting from the assumptions made in the fit model and analysis methods (in this case an alternative hypothesis is tested, and the fit to the data sample is repeated).
The several parameters of interest are measured and their values are provided in the Tab. 2. All main physics parameters of interest are found to be consistent with the SM-based predictions [28] as well as with the world-averaged values [16]. The measured value of $|\lambda|$ is consistent with no direct CP violation.

Table 2. Results of the fit to data for the main physics parameters [13].

Parameter	Fit value	Stat. uncer.	Syst. uncer.
ϕ_s[mrad]	-73	±23	±7
$\Delta\Gamma_S \left[\text{ps}^{-1}\right]$	0.0761	±0.0043	±0.0019
$\Gamma_s \left[\text{ps}^{-1}\right]$	0.6613	±0.0015	±0.0028
$\Delta m_s \left[\hbar\text{ps}^{-1}\right]$	17.757	±0.035	±0.017
$\lvert\lambda\rvert$	1.011	±0.014	±0.012
$\lvert A_0\rvert^2$	0.5300	±0.0016	±0.0044
$\lvert A_\perp\rvert^2$	0.2409	±0.0021	±0.0030
$\lvert A_S\rvert^2$	0.0067	±0.0033	±0.0009
$\delta_\parallel$	3.145	±0.074	±0.025
$\delta_\perp$	2.931	±0.089	±0.050
$\delta_{S\perp}$	0.48	±0.15	±0.05

The results obtained with Run 2 data are further combined with those obtained by CMS at $\sqrt{s} = 8$TeV [28]. The combined result [13] for the CP-violating phase is $\phi_s = -74 \pm 23$mrad, while for the decay width difference is $\Delta\Gamma_s = 0.0780 \pm 0.0045\text{ps}^{-1}$, both values are consistent with the SM-based predictions. The 2D ϕ_s vs. $\Delta\Gamma_s$ contours for one, two, and three s.d. for the combined results, as well as the SM prediction, are shown in Fig. 7. The combined ϕ_s value exhibits a deviation from zero by 3.2 s.d., providing the first evidence for CPV in $\text{B}_\text{s}^0 \to \text{J}/\psi\text{K}^+\text{K}^-$decays.

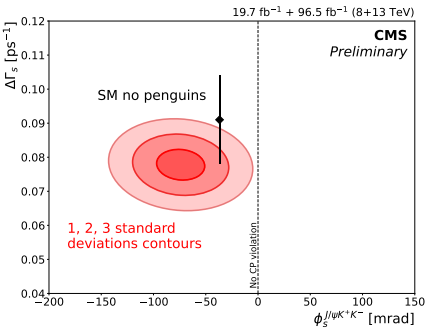

Figure 7. The two-dimensional one, two, and three s.d. contours in the $\phi_s - \Delta\Gamma_s$ plane for the combined results. Both statistical and systematic uncertainties are taken into account. The SM prediction is represented by the black rectangle, with the central value indicated with the black diamond [2, 3, 63]. The dashed line indicates no CPV in the B_s^0 meson decay/mixing interference [13].

5 Conclusion

The CMS detector recent contributions to flavor physics prove that it can be one of the leading actors in such areas as rare decays, spectroscopy, and, likewise, precision measurements of CP violation parameters. All these results are possible due to refined trigger strategies, as well as the advanced methods of tagging. The CMS Run 3 data will provide unique opportunities thanks of a revamped trigger strategy, which will lead to the collection of an unprecedented amount of data suitable for flavor physics studies.

6 Acknowledgements

The author would like to acknowledge the FPCP 2024 organizing committee for the important opportunity to give the present talk at the conference, which is an important boost in the career of young scientist. The author's work was supported by the Russian Scientific Foundation grant № 24-22-00445.

References

[1] A. D. Sakharov, Violation of CP invariance, C asymmetry, and baryon asymmetry of the universe. Pisma Zh. Eksp. Teor. Fiz. **5**, p. 32–35 (1967). http://dx.doi.org/10.1070/PU1991v034n05ABEH002497

[2] N. Cabibbo et al., Unitary symmetry and leptonic decays. Phys. Rev. Lett. **10**, p. 531–533 (1963). http://dx.doi.org/10.1103/PhysRevLett.10.531

[3] M. Kobayashi and T. Maskawa, CP-violation in the renormalizable theory of weak interaction. Prog. Theor. Phys. **49**, p. 652–657 (1973). http://dx.doi.org/10.1103/PhysRevLett.10.531

[4] A. G. Cohen, D. B. Kaplan, and A. E. Nelson, Progress in electroweak baryogenesis. Ann. Rev. Nucl. Part. Sci.**43**, p. 27–70 (1993). http://dx.doi.org/10.1146/annurev.ns.43.120193.000331

[5] CMS Collaboration, The CMS experiment at the CERN LHC. JINST **3**, (2008) S08004. https://doi.org/10.1088/1748-0221/3/08/S08004

[6] CMS Collaboration, CMS tracking performance results from early LHC operation. Eur. Phys. J. C **70**, (2010). https://doi.org/10.1140/epjc/s10052-010-1491-3

[7] CMS Collaboration, Measurement of the $B_s^0 \to \mu^+\mu^-$ decay properties and search for the $B^0 \to \mu^+\mu^-$ decay in proton-proton collisions at $\sqrt{s} = 13$ TeV. Phys. Lett. B. **842**, (2023). https://doi.org/10.1016/j.physletb.2023.137955

[8] CMS Collaboration, Observation of the Rare Decay of the η Meson to Four Muons. Phys. Rev. Lett. **131**, (2023). https://doi.org/10.1103/PhysRevLett.131.091903

[9] CMS Collaboration, Observation of a New Excited Beauty Strange Baryon Decaying to $\Xi_b^-\pi^+\pi^-$. Phys. Rev. Lett. **126**, (2021). https://doi.org/10.1103/PhysRevLett.126.252003

[10] CMS Collaboration, New Structures in the $J/\psi J/\psi$ Mass Spectrum in Proton-Proton Collisions at $\sqrt{s} = 13$ TeV. Phys. Rev. Lett. **132**, (2024).

[11] CMS Collaboration, Search for CP violation in $D^0 \to K_S^0 K_S^0$ decays in proton-proton collisions at $\sqrt{s} = 13$ TeV. Submitted to Eur. Phys. J. C, (2024). https://doi.org/10.48550/arXiv.2405.11606

[12] CMS Collaboration, Measurement of the B_s^0 effective lifetime in the decay $B_s^0 \to J/\psi K_S^0$ from pp collisions at $\sqrt{s} = 13$ TeV. CMS-PAS-BPH-22-001, (2024). https://cms-results.web.cern.ch/cms-results/public-results/preliminary-results/BPH-22-001/

[13] CMS Collaboration, Measurement of time-dependent CP violation in $B_s^0 \to J/\psi\phi(1020)$ decays with the CMS detector. CMS-PAS-BPH-23-004, (2024). https://cms-results.web.cern.ch/cms-results/public-results/preliminary-results/BPH-23-004/

[14] S. L. Glashow, J. Iliopoulos, and L. Maiani, Weak interactions with lepton-hadron symmetry. Phys. Rev. D. **2**, p. 1285–1292 (1970). https://doi.org/10.1103/PhysRevD.2.1285.

[15] U. Nierste and S. Schacht, CP violation in $D^0 \to K_S^0 K_S^0$. Phys. Rev. D. **92**, (2015). http://doi.org/10.1103/PhysRevD.92.054036

[16] Particle Data Group, Review of particle physics. PTEP **2022**, (2022). http://doi.org/10.1093/ptep/ptac097

[17] LHCb Collaboration, Measurement of CP asymmetry in in $D^0 \to K_S^0 K_S^0$. Phys. Rev. D. **104**, (2021). http://doi.org/10.1103/PhysRevD.104.L031102

[18] CMS Collaboration, Enriching the physics program of the CMS experiment via data scouting and data parking, (2024) https://arxiv.org/abs/2403.16134

[19] Heavy Flavor Averaging Group Collaboration, Averages of b-hadron, c-hadron, and τ-lepton properties as of 2021. Phys. Rev. D. **107**, (2023). http://doi.org/10.1103/PhysRevD.107.052008

[20] K. De Bruyn, R. Fleischer, and P. Koppenburg, Extracting γ and Penguin Topologies through CP Violation in $B_s^0 \to J/\psi K_S^0$. Eur. Phys. J. C. **70**, (2010). http://doi.org/10.1140/epjc/s10052-010-1495-z

[21] LHCb Collaboration, Measurement of the effective $B_s^0 \to J/\psi K_S^0$ lifetime. Nucl. Phys. B. **873**, (2013). http://doi.org/10.1016/j.nuclphysb.2013.04.021

[22] CMS Collaboration, Precision luminosity measurement in proton-proton collisions at $\sqrt{s} = 13$ TeV in 2015 and 2016 at CMS. Eur. Phys. J. C. **81**, (2021). https://doi.org/10.1140/epjc/s10052-021-09538-2

[23] P. B. Rodríguez et al.,Calibration of the momentum scale of a particle physics detector using the Armenteros-Podolanski plot. JINST. **16**, (2021). https://doi.org/10.1088/1748-0221/16/06/P06036

[24] L.-G. Xia, Understanding the boosted decision tree methods with the weak-learner approximation, (2018) https://arxiv.org/abs/1811.04822

[25] A. S. Dighe, I. Dunietz, H. J. Lipkin, and J. L. Rosner, Angular distributions and lifetime differences in $B_s^0 \to J/\psi\phi$. Phys. Lett. B. **369**, (1996). https://doi.org/10.1016/0370-2693(95)01523-X

[26] F. Chollet et al., Keras, (2015) https://keras.io/

[27] D. Kingma and J. Ba, Adam: a method for stochastic optimization. International Conference on Learning Representations (2014) https://arxiv.org/abs/1412.6980

[28] The CKMfitter Group Collaboration, Predictions of selected flavour observables within the Standard Model. Phys. Rev. D. **84**, (2011). http://doi.org/10.1103/PhysRevD.84.033005